some waveguide discontinuity problems, IEEE Trans Microwave Theory Tech MTT-18 (1970), 364–369.
13. H. Ikuno and K. Yasuura, Improved point-matching method with application to scattering from a periodic surface, IEEE Trans Antennas and Propagation AP-21 (1973), 657–662.
14. R.E. Collin, Field Theory of Guided Waves, IEEE Press, 1991.

HIGHER-ORDER HIERARCHICAL BASIS FUNCTIONS WITH IMPROVED ORTHOGONALITY PROPERTIES FOR MOMENT-METHOD MODELING OF METALLIC AND DIELECTRIC MICROWAVE STRUCTURES

Miroslav Djordjević and Branislav M. Notaroš
University of Massachusetts Dartmouth
Department of Electrical and Computer Engineering
285 Old Westport Road
Dartmouth, MA 02747-2300

Received 10 October 2002

ABSTRACT: *Three classes of higher-order hierarchical basis functions, constructed from standard orthogonal polynomials, are proposed and evaluated for the modeling of combined metallic and dielectric microwave structures. The reduction of the condition number of moment-method matrices is several orders of magnitude, as compared to the technique using regular polynomial basis functions.*
© 2003 Wiley Periodicals, Inc. Microwave Opt Technol Lett 37: 83–88, 2003; Published online in Wiley InterScience (www.interscience.wiley.com). DOI 10.1002/mop.10831

Key words: *moment method; higher-order basis functions; condition number; electromagnetic scattering*

1. INTRODUCTION

The method of moments (MoM) for discretizing integral equations in electromagnetics [1] is an extremely powerful and versatile general numerical methodology for electromagnetic-field simulation in RF and microwave applications. In this paper, we concentrate on surface-integral-equation (SIE) methods in the frequency domain. We address the SIE analysis of combined metallic and dielectric structures (antennas and scatterers), where both electric and magnetic surface currents are introduced over boundary surfaces between homogeneous parts of the structure, and integral equations based on boundary conditions for both electric and magnetic field intensity vectors are solved with current densities as unknowns [2, 3]. Furthermore, this paper focuses on higher-order basis functions for current approximation which constitute the large-domain (entire-domain) MoM approach [3].

For the modeling of all the surfaces in the system (metallic and dielectric surfaces), we use bilinear quadrilaterals with divergence-conforming hierarchical polynomial basis functions of local parametric coordinates, which are developed by modifying simple power functions so that the current-continuity condition across the quadrilateral edges is automatically satisfied. Polynomial degrees in the current expansions can be high (higher-order expansions), so that electrically large surface elements can be used (large-domain method). For instance, the size of patches in the model can be as large as 2λ in each dimension, where λ is the wavelength in the medium [3]. This greatly reduces the overall number of unknowns for a given problem and significantly enhances the accuracy and efficiency of the technique, as compared to the traditionally used low-order basis functions and small-domain (subdomain) methods [2], where all the patches must be less than approximately $\lambda/10$ in each dimension.

Polynomial basis functions adopted for implementation in this paper are hierarchical functions, that is, each lower-order set of functions is a subset of all higher-order sets. These functions enable different orders of current approximation over different quadrilaterals to be used, which thereby allows a whole spectrum of quadrilateral sizes (from a very small fraction of λ to a couple of λ) and the corresponding current approximation orders to be used at the same time in a single simulation model of a complex structure. Additionally, each individual quadrilateral can have drastically different edge lengths, thus enabling a whole range of quadrilateral shapes (such as square-shaped, rectangular, trapezoidal, triangle-like, strip-like, etc.) to be used in a simulation model as well. Hierarchical basis functions, on the other hand, generally have poor orthogonal properties, which results in MoM matrices with large condition numbers. This affects the overall accuracy and stability of the solution. Most importantly, if the linear equations associated with the MoM are solved using iterative solvers, the overall computation time is much larger when the MoM matrices are badly conditioned (for example the number of iterations for conjugate gradient solvers is proportional to the square root of the condition number).

The novelty of higher-order basis functions, in general, and the dilemmas involved in actually using them are tremendously interesting and relevant to computational electromagnetics (CEM). Problems with the ill-conditioning of the system matrices probably represent the most important issue in higher-order CEM, especially if hierarchical bases are used. However, only a very limited number of publications [4–8] have addressed these problems within the framework of either the finite element method (FEM) or MoM.

This paper presents investigations that aim to improve the orthogonality properties of polynomial higher-order hierarchical basis functions, leading to better conditioned MoM matrices and more stable solutions in SIE modeling. Four different types of polynomial basis functions are implemented in the large-domain Galerkin SIE method to enable cross-validation of the results and comparison of numerical properties of the four sets of basis functions. Some preliminary results of this research are presented in [6, 7]. We show that by combining the simple 2D power functions of parametric coordinates in accordance with standard orthogonal polynomials (namely, ultraspherical and Chebyshev polynomials), and modifying them so that the current-continuity condition across the quadrilateral edges is automatically satisfied (divergence-conforming functions), higher-order polynomial basis functions are obtained. These functions lead to much better conditioned matrices as compared to the "regular" higher-order polynomial basis functions we have used so far in the volume-integral-equation (VIE) MoM [9], SIE MoM [3], and FEM [10]. The polynomials are combined in different ways for representing variations of the current density vector over quadrilateral patches in the direction along the vector (this variation is relevant for the functions' divergence conformity) and across the vector, and the resulting basis functions and corresponding versions of the MoM code are evaluated. Generally, the new basis functions yield a reduction of the MoM matrix condition number of several orders of magnitude. However, this improvement is less pronounced in analyses of surfaces with curvature and of dielectric (penetrable) structures.

2. SURFACE INTEGRAL EQUATION FORMULATION

Consider a metallic/dielectric structure situated in a vacuum and excited by a time-harmonic incident electromagnetic field of angular frequency ω. According to the surface equivalence principle [3], we can break the entire system into subsystems, each representing one of the dielectric regions (domains), together with their metallic surfaces, with the remaining space being filled with the same medium. The scattered electric and magnetic fields in each domain can be expressed in terms of the equivalent surface electric and magnetic currents $\boldsymbol{J}_S$ and $\boldsymbol{M}_S$, which are placed on the boundary surface S of the domain, with the objective to produce a zero total field in the surrounding space, given by

$$\boldsymbol{E} = -j\omega\boldsymbol{A} - \nabla\Phi - \frac{1}{\varepsilon}\nabla\times\boldsymbol{F}, \quad \boldsymbol{H} = -j\omega\boldsymbol{F} - \nabla U + \frac{1}{\mu}\nabla\times\boldsymbol{A}, \tag{1}$$

$$\boldsymbol{A} = \mu\int_S \boldsymbol{J}_S g dS,$$

$$\boldsymbol{F} = \varepsilon\int_S \boldsymbol{M}_S g dS,$$

$$\Phi = \frac{j}{\omega\varepsilon}\int_S \nabla_S\cdot\boldsymbol{J}_S g dS,$$

$$U = \frac{j}{\omega\mu}\int_S \nabla_S\cdot\boldsymbol{M}_S g dS,$$

$$g = \frac{e^{-\gamma R}}{4\pi R}, \tag{2}$$

where g is the Green's function for the unbounded homogeneous medium of complex parameters ε and μ, $\gamma = j\omega\sqrt{\varepsilon\mu}$, and R is the distance of the field point from the source point. The boundary conditions for the tangential components of the total (incident plus scattered) electric and magnetic field vectors on the boundary surface between any two adjacent dielectric domains yield a set of coupled electric/magnetic field integral equations (EFIE/MFIE) for $\boldsymbol{J}_S$ and $\boldsymbol{M}_S$ as unknowns.

As a basic building block for geometry modeling, we adopt a bilinear quadrilateral [3], defined by

$$\boldsymbol{r}(u, v) = \boldsymbol{r}_c + \boldsymbol{r}_u u + \boldsymbol{r}_v v + \boldsymbol{r}_{uv} uv, \quad -1 \le u, v \le 1, \tag{3}$$

where $\boldsymbol{r}_c$, $\boldsymbol{r}_u$, $\boldsymbol{r}_v$, and $\boldsymbol{r}_{uv}$ are constant vectors that can be expressed in terms of the position vectors of the quadrilateral vertices. The surface current density vectors over quadrilaterals are represented as [3]:

$$\boldsymbol{J}_S(u, v) = \frac{1}{J(u, v)} \times \left(\sum_{i=0}^{N_u}\sum_{j=0}^{N_v-1}\alpha_{uij}f_{uij}(u, v)\boldsymbol{a}_u(v) + \sum_{i=0}^{N_u-1}\sum_{j=0}^{N_v}\alpha_{vij}f_{vij}(u, v)\boldsymbol{a}_v(u)\right), \tag{4}$$

$$J(u, v) = |\boldsymbol{a}_u(v)\times\boldsymbol{a}_v(u)|, \quad \boldsymbol{a}_u(v) = \frac{d\boldsymbol{r}(u, v)}{du}, \quad \boldsymbol{a}_v(u) = \frac{d\boldsymbol{r}(u, v)}{dv}, \tag{5}$$

with analogous representation for $\boldsymbol{M}_S(u, v)$, where f are divergence-conforming hierarchical polynomial basis functions of coordinates u and v, N_u and N_v are the adopted degrees of the polynomial approximation, and α_{uij} and α_{vij} are unknown current-distribution coefficients. Note that the sum limits in Eq. (4) that correspond to the variations of a current density vector component in the direction across that component are smaller (by one order) than the orders corresponding to the variations in the other parametric coordinate. This mixed-order arrangement has been found to be a preferable choice, in terms of accuracy and efficiency, for modeling of surface currents in all applications. In order to determine the unknown coefficients $\{\alpha\}$, the EFIE/MFIE system is tested using the same functions used for the current expansion (Galerkin-type MoM).

3. THE CHOICE OF BASIS FUNCTIONS

The first class of analyzed basis functions is a set of simple 2D polynomial functions in the $u - v$ coordinate system that automatically satisfy the current-continuity condition for the normal components of $\boldsymbol{J}_S$ and $\boldsymbol{M}_S$ along an edge shared by quadrilateral elements (divergence conformity) and actually represent a higher-order generalization of traditionally used rooftop functions. These functions, hereafter referred to as the regular polynomials, are given by [3]:

$$f_{uij}(u, v) = \left\{\begin{array}{ll} 1-u, & i=0 \\ u+1, & i=1 \\ u^i-1, & i\ge 2,\text{ even} \\ u^i-u, & i\ge 3,\text{ odd}\end{array}\right\} v^j \quad \text{(regular polynomials)} \tag{6}$$

with an analogous expression for $f_{vij}(u, v)$. The basis functions $(1 - u)v^j$ (for $i = 0$) and $(u + 1)v^j$ (for $i = 1$) in an arbitrary quadrilateral serve for adjusting the continuity condition on the side $u = -1$ and $u = 1$, respectively, while the remaining basis functions (for $i \ge 2$) are zero at the quadrilateral edges and serve for improving the current approximation over the surface. Similar functions are used in the large-domain VIE MoM [9] and FEM [10].

We note that, as the polynomial degrees N_u and N_v in Eq. (4) increase, the basis functions in Eq. (6) become increasingly similar to one another and, consequently, the condition number of the MoM matrix built from them deteriorates. The ill-conditioning is principally caused by a strong mutual coupling between the pairs of higher-order functions defined on the same (electrically large) bilinear patch. In order to reduce this coupling (and thus improve the condition number of the resulting MoM matrix), basis functions with better orthogonal properties have to be utilized. Due to their simplicity and flexibility, standard orthogonal polynomials [11] (and their modifications) are adopted as candidate basis functions in this paper. In one dimension, these functions are defined as classes of polynomials $p_n(x)$ of the interval $[-1, 1]$, satisfying the orthogonality relationship

$$\int_{-1}^{1} w(x)p_m(x)p_n(x)dx = \delta_{mn}c_n, \tag{7}$$

where $w(x)$ is a weighting function and δ_{mn} is the Kronecker delta.

Note that all the classes of orthogonal polynomials for all polynomial orders n have nonzero values for $x = \pm 1$ (all the zeros of the polynomials lie in the interior of the interval $[-1, 1]$), which makes the two-dimensional form of these functions not divergence-conforming and not directly applicable to the higher-order Galerkin SIE method in the fashion suggested by Eq. (4). Note also that the integral kernels of Galerkin generalized impedances based on Eqs. (1) and (2) contain the Green's function g as a "weighting function" in the inner product, which, of course, cannot be reproduced by combining the function $w(x)$ for any of the orthogonal polynomials. These are the two basic problems that need to be addressed with regard to the actual implementation of standard orthogonal polynomials in the higher-order MoM.

So-called ultraspherical polynomials [11] are orthogonal on the interval $[-1, 1]$ with the weighting function $w(x) = (1 - x^2)^{\alpha - 1/2}$, where $\alpha > -1/2$. For $\alpha = -1/2$, the relationship in Eq. (7) is not satisfied exactly, but the polynomials have zero values for $x = \pm 1$ and $n \geq 2$. Hence, the ultraspherical polynomials with $\alpha = -1/2$, although only partially orthogonal to one another, represent an attractive basis for constructing divergence-conforming 2D polynomial current expansions. Thus, the second class of divergence-conforming hierarchical MoM basis functions proposed for implementation and investigation in this paper is constructed as

$$f_{uij}(u, v) = \begin{Bmatrix} 1 - u, & i = 0 \\ u + 1, & i = 1 \\ P_i(u), & i \geq 2 \end{Bmatrix} P_j(v)$$

(ultraspherical/ultraspherical polynomials)

$$P_0(x) = 1, \quad P_1(x) = -x,$$
$$nP_n(x) = (2n - 3)xP_{n-1}(x) - (n - 3)P_{n-2}(x), \quad (8)$$

analogously for $f_{vij}(u, v)$.

Another attractive basis for constructing current expansions with improved orthogonality is the class of Chebyshev polynomials [11]; this is because, out of all weighting functions with respect to which individual standard polynomials are orthogonal, the one with Chebyshev polynomials of the first kind, $w(x) = (1 - x^2)^{-1/2}$, most closely resembles the 1D version of the Green's function in Eq. (2). Furthermore, for these polynomials, all the maxima are equal to 1 and minima are equal to -1, which also adds to their flexibility for approximating the current variations on the interval $[-1, 1]$ and their overall suitability for implementation in the SIE technique. However, Chebyshev polynomials are nonzero at the interval boundaries and therefore cannot be directly used for representing the variation of the current density vectors $\boldsymbol{J}_S$ and $\boldsymbol{M}_S$ over quadrilateral patches in the direction along the vectors. Hence, the third class of proposed basis functions for the u component of current density vectors incorporates the Chebyshev polynomials in the v coordinate (this variation is not relevant for divergence-conformity of functions), yielding the following combined ultraspherical/Chebyshev 2D polynomial basis functions:

$$f_{uij}(u, v) = \begin{Bmatrix} 1 - u, & i = 0 \\ u + 1, & i = 1 \\ P_i(u), & i \geq 2 \end{Bmatrix} T_j(v),$$

(ultraspherical/Chebyshev polynomials)

$$T_0(x) = 1, \quad T_1(x) = x, \quad T_n(x) = 2xT_{n-1}(x) - T_{n-2}(x). \quad (9)$$

Similar expressions are constructed for the v component of the vectors.

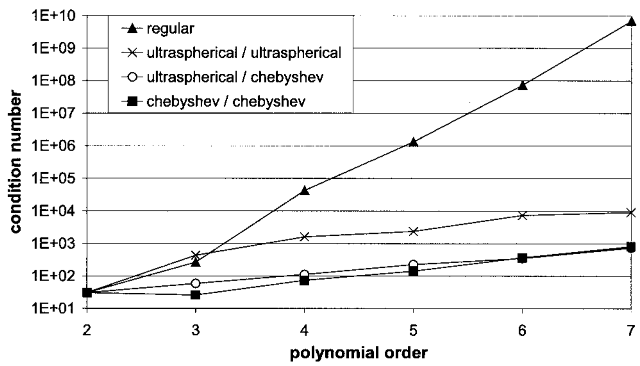

Figure 1 Condition number of the MoM matrix for a square metallic plate scatterer (edge length $a = 1$ m, frequency range 43–376 MHz), as a function of the current approximation order in one dimension, for four classes of basis functions

Finally, the fourth class of analyzed basis functions is constructed entirely from Chebyshev polynomials, which have been combined in the following way, (similar to that in [8]), to ensure the divergence-conformity of the expansions:

$$f_{uij}(u, v) = \begin{Bmatrix} 1 - u, & i = 0 \\ u + 1, & i = 1 \\ T_i(u) - T_{i-2}(u), & i \geq 2 \end{Bmatrix} T_j(v),$$

(Chebyshev/Chebyshev polynomials). (10)

Note that using the difference of the polynomials of orders i and $i - 2$ as the basis function of order i in approximating the variation of the current density vectors along the u coordinate (or, in general, in the direction along the vectors) makes the higher-order expansions zero across the edges shared by adjacent quadrilaterals and allows for the maximum number of basis functions to be mutually orthogonal with respect to the corresponding 2D weighting function $w(u, v) = (1 - u^2)^{-1/2}(1 - v^2)^{-1/2}$.

4. NUMERICAL RESULTS

As the first numerical example, consider a square plate metallic scatterer with sides of 1 m. The scatterer is analyzed from 43 MHz to 376 MHz, with the plate modeled as a single bilinear quadrilateral and current approximation orders ranging from $N_u = N_v = 2$ (4 unknowns) to $N_u = N_v = 7$ (84 unknowns). Figure 1 shows the condition number of the MoM matrix for the scatterer, as a function of the current approximation order in one dimension ($N_u = N_v$), obtained by using the four types of basis functions. We observe that the use of regular polynomial basis functions, Eq. (6), yields a severely ill-conditioned MoM matrix, with the condition number rapidly increasing as the current approximation order increases. On the other hand, using the novel types of basis functions, Eqs. (8)–(10), the increase of the condition number caused by the increase of the approximation order is much slower. Specifically, the use of ultraspherical/ultraspherical basis functions reduces the condition number at the highest frequency more than 750,000 times, whereas the reduction of the condition number using ultraspherical/Chebyshev and Chebyshev/Chebyshev basis functions is almost 10^7 times, as compared to the regular polynomials at the highest frequency.

As another example of metallic structures with flat surfaces, consider a cube metallic scatterer of edge length $a = 1$ m. The frequency is varied from 100 MHz to 1.6 GHz and the number of unknowns from 48 to 3888, respectively. Each side of the cube is

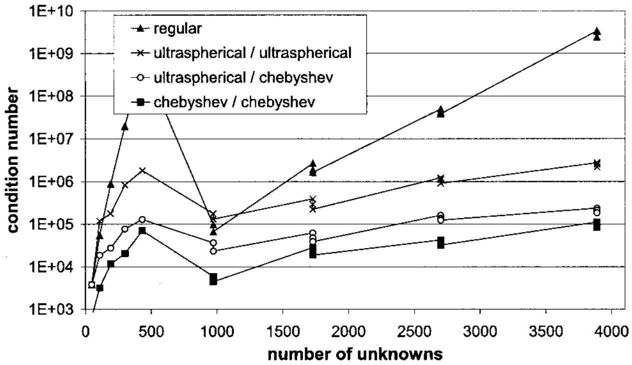

Figure 2 Condition number of the MoM matrix for a cube metallic scatterer (edge length $a = 1$ m, frequency range 100 MHz–1.6 GHz), as a function of the number of unknowns, for four classes of basis functions

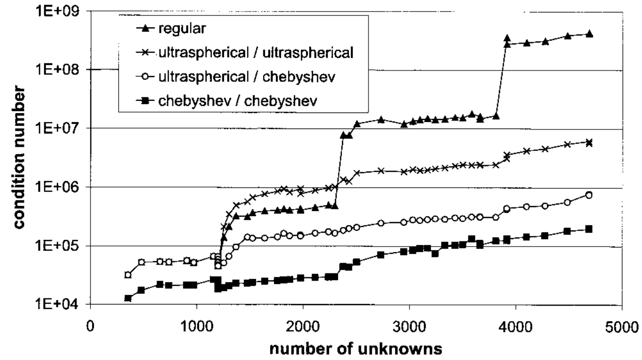

Figure 4 Condition number of the MoM matrix for a spherical metallic scatterer (radius $a = 1$ m, frequency range 10–600 MHz) for four classes of basis functions

modeled by a single bilinear quadrilateral at frequencies below 600 MHz and by nine quadrilaterals at higher frequencies. Figure 2 shows the condition number of the MoM matrix as a function of the number of unknowns, for the four types of analyzed basis functions. We observe that the use of ultraspherical/ultraspherical, ultraspherical/Chebyshev, and Chebyshev/Chebyshev basis functions provides the reduction of the condition number of approximately 1100, 13000, and 29000 times, respectively, as compared to regular polynomials at the highest frequency.

As an example of curved metallic structures, consider a spherical metallic scatterer of radius $a = 1$ m, modeled by 600 curved bilinear quadrilaterals. The frequency range is 10–600 MHz and the number of unknowns is 300 to 4,686, using two-fold symmetry. At the highest frequency, polynomial current approximation orders are 3, 4, and 5, over quadrilateral patches of different sizes. The radar cross section (RCS) predictions obtained using the four types of basis functions appear to be practically identical, and agree well with the analytical solution in the form of Mie's series, as shown in Figure 3. Figure 4 shows the condition number of the MoM matrix for the sphere obtained using different basis functions. We observe that all the sets of basis functions constructed from orthogonal polynomials yield a significant reduction of the condition number, as compared to regular polynomial basis functions; the reduction with Chebyshev/Chebyshev basis functions is larger than 2000 times. However, the improvement in the condition number using novel basis functions is less pronounced than that achieved by analyzing structures with flat surfaces. This may be attributed primarily to the additional coupling between surface current density components defined on curved bilinear patches and also to the fact that the model consists of a large number of patches with relatively low current approximation orders (quasi-subdomain approximation) needed for the sphere surface to be accurately geometrically represented.

As an example of dielectric structures with flat surfaces, consider a dielectric cube of edge length 1 m and relative permittivity $\varepsilon_r = 2.25$. The cube is analyzed as a scatterer from 100 MHz to 1000 MHz, and modeled by 6 (up to 500 MHz) or 54 bilinear quadrilateral patches. The polynomial current approximation orders range from 2 to 7 and the number of unknowns ranges from 96 to 5400, respectively. Figure 5 shows the MoM matrix condition number as a function of the number of unknowns, for the four types of analyzed basis functions. As can be observed, the full coupled system of integral equations for dielectric structures produces extremely ill-conditioned MoM matrices. While the improvement in the condition number using novel basis functions is significant (the reduction at the highest frequency is 1100 times with Chebyshev/Chebyshev basis functions, as compared to regular polynomials), it is not that dramatic as in the case of the metallic cube. This may be attributed primarily to the additional coupling between electric and magnetic surface currents defined on the same electrically large bilinear patch.

As an example of curved dielectric structures, consider a spherical dielectric ($\varepsilon_r = 2.25$) scatterer, 1 m in radius and modeled by 384 curved quadrilaterals with polynomial current approximation orders 1, 2, and 3 in the frequency range 10–600 MHz. Using two-fold symmetry, the number of unknowns ranges from 384 to 2904. The RCS results obtained by the large-domain MoM (all

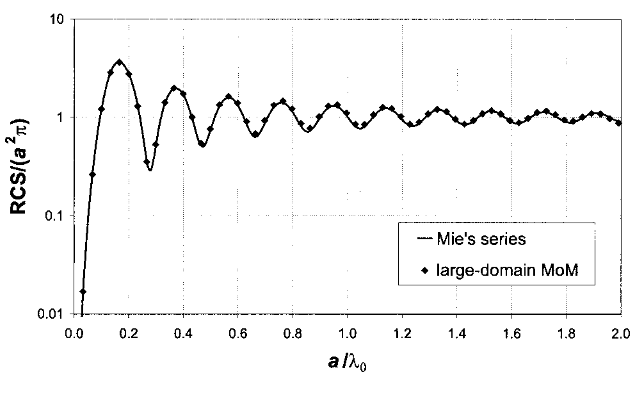

Figure 3 Radar cross section of a metallic sphere: large-domain MoM solution and analytical solution

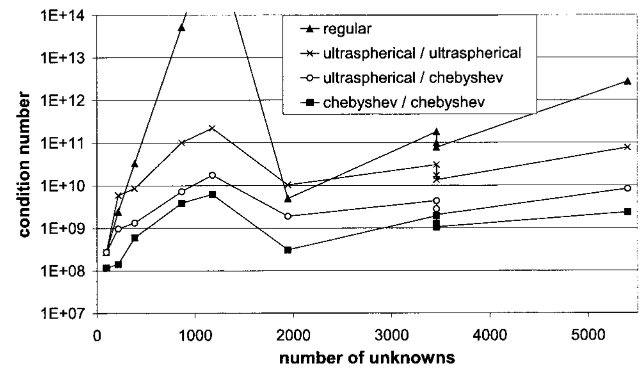

Figure 5 Condition number of the MoM matrix for a dielectric cube scatterer (edge length $a = 1$ m, relative permittivity $\varepsilon_r = 2.25$, frequency range 100–1000 MHz) for four classes of basis functions

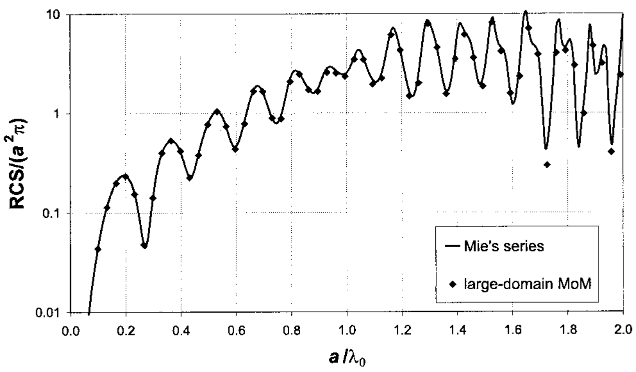

Figure 6 Radar cross-section of a dielectric sphere ($\varepsilon_r = 2.25$): large-domain MoM solution and analytical solution

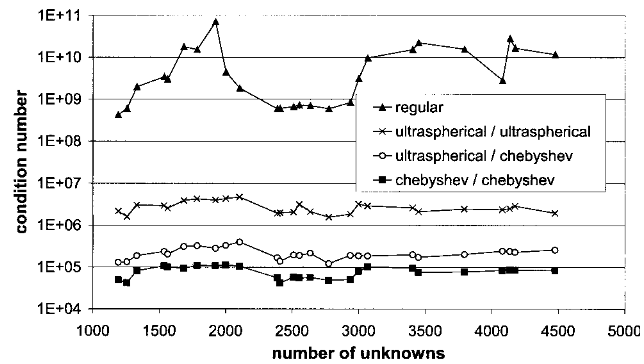

Figure 8 Condition number of the MoM matrix for the vehicle model in Fig. 7 with an interior antenna (frequency range 500–1000 MHz) for four classes of basis functions

four sets of basis functions yield practically identical solutions) agree well with the analytical solution in the form of Mie's series, as shown in Figure 6. However, it is found that the reduction of the MoM matrix condition number using novel basis functions is considerably smaller (the reduction with Chebyshev/Chebyshev basis functions is only 15 times as compared to regular polynomials at the highest frequency) than in cases of the dielectric cube and metallic sphere. Generally, this is characteristic to all curved and/or dielectric structures.

Finally, as an example of complex real-life structures, consider a vehicle (Golf GL) with a cellular-telephone antenna (situated inside) in the frequency range 500–1000 MHz [12]. Figure 7 shows the simulated geometrical model of the vehicle. The number of bilinear quadrilaterals in the model ranges from 162 to 354 and the number of unknowns using symmetry ranges from 1191 to 4475, respectively. Figure 8 shows the condition number of the MoM matrix as a function of the number of unknowns, obtained by the four sets of higher-order basis functions. We observe that the use of ultraspherical/ultraspherical basis functions yields the reduction ranging from 200 to 18000 times, as compared to regular polynomial basis functions. Ultraspherical/Chebyshev basis functions provide approximately further 15-fold reduction. Finally, Chebyshev/Chebyshev basis functions perform the best, yielding a reduction range of 8700 to 650000 times, with respect to regular polynomials in the considered frequency range.

5. CONCLUSION

This paper has presented investigations that aim to improve the orthogonal properties of polynomial higher-order hierarchical basis functions, leading to better conditioned MoM matrices in frequency-domain surface-integral-equation modeling of combined metallic and dielectric RF/microwave structures. The metallic and dielectric surfaces are modeled by electrically large bilinear quadrilaterals (up to 2λ in each dimension) with divergence-conforming higher-order expansions (up to the 10th order) for electric and magnetic surface current density vectors. The EFIE/MFIE system is tested using the Galerkin method. Four different types of polynomial basis functions are implemented in the same method, yielding four independent versions of the MoM code. The results obtained using the four sets of basis functions appear to be practically identical, and agree well with available analytical solutions. Combinations of basis functions constructed from standard orthogonal polynomials, both ultraspherical and Chebyshev types, yield the reduction of the MoM matrix condition number of several orders of magnitude (for example, 4 to 7 orders of magnitude with the use of Chebyshev/Chebyshev basis functions for metallic structures with flat surfaces), as compared to the technique using regular polynomial basis functions. However, although significant, the improvement of the conditioning of the MoM matrix using novel basis functions is considerably less pronounced in the analyses of surfaces with curvature and of dielectric structures (for example, 1 to 2 orders of magnitude using Chebyshev/Chebyshev functions for curved dielectric structures).

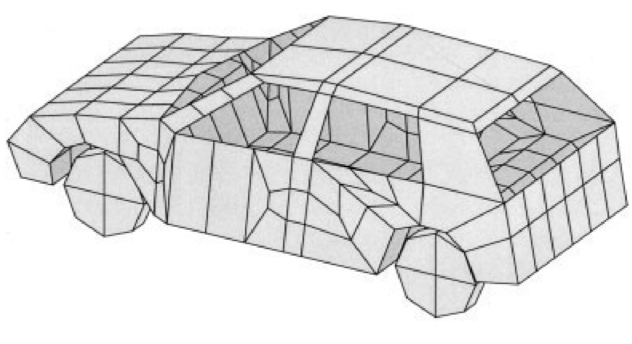

Figure 7 Large-domain MoM geometrical model of a vehicle (Golf GL) at 860 MHz

ACKNOWLEDGEMENT

This work was supported by the National Science Foundation under grant no. ECS-0115756.

REFERENCES

1. R.F. Harrington, Field computation by moment methods, Macmillan, New York, 1968.
2. J.S. Shin, A.W. Glisson, and A.A. Kishk, Analysis of combined conducting and dielectric structures of arbitrary shapes using an E-PMCHW integral equation formulation, 2000 IEEE Antennas Propagat Soc Int Symp Dig, Salt Lake City, UT, 2000, pp. 2282–2285.
3. B.M. Notaros, B.D. Popovic, J. Peeters Weem, R.A. Brown, and Z. Popovic, Efficient large-domain MoM solution to electrically large practical EM problems, IEEE Trans Microwave Theory Tech 49 (2001), 151–159.
4. L.S. Andersen and J.L. Volakis, Condition numbers for various FEM matrices, J Electromagn Waves Appl 13 (1999), 1663–1679.
5. J.P. Webb, Hierarchical vector basis functions of arbitrary order for triangular and tetrahedral finite elements, IEEE Transactions on Antennas and Propagation 47 (1999), 1244–1253.
6. M. Djordjevic and B.M. Notaros, Three types of higher-order MoM basis functions automatically satisfying current continuity conditions, 2002 IEEE Antennas Propagat Soc Int Symp Dig, San Antonio, TX, 2002, pp. IV.610–613.

7. B.M. Notaros, B.D. Popovic, M. Djordjevic, and M.M. Ilic, Hierarchical and interpolatory higher-order vector basis functions for finite element method and method of moments, 6th International Workshop on Finite Elements for Microwave Engineering, Antennas, Circuits and Devices—Book of Abstracts, Chios, Greece, 2002, p. 65.
8. E. Jorgensen, J.L. Volakis, P. Meincke, and O. Breinbjerg, Higher order hierarchical Legendre basis functions for iterative integral equation solvers with curvilinear surface modeling, 2002 IEEE Antennas Propagat Soc Int Symp Dig, San Antonio, TX, 2002, pp. IV.618–621.
9. B.M. Notaros and B.D. Popovic, Large-domain integral-equation method for analysis of general 3D electromagnetic structures, IEE Proceedings—Microwaves, Antennas and Propagation 145 (1998), 491–495.
10. M.M. Ilic and B.M. Notaros, Computation of 3-D electromagnetic cavity resonances using hexahedral vector finite elements with hierarchical polynomial basis functions, 2002 IEEE Antennas Propagat Soc Int Symp Dig, San Antonio, TX, 2002, pp. IV.682–685.
11. M. Abramowitz and C.A. Stegun (Eds.), Handbook of Mathematical Formulas, Graphs and Mathematical Tables, Ch. 22 Orthogonal Polynomials, New York-Dover, 1972, pp. 771–802.
12. M. Djordjevic and B.M. Notaros, Highly efficient large-domain moment-method analysis and CAD of radio-frequency antennas mounted on or situated in vehicles, Fall 2000 IEEE Vehicular Technology Conference Digest, Boston, MA, 2000, pp. 2373–2377.

LEAKY AND SURFACE WAVES IN MULTILAYERED LATERALLY-SHIELDED MICROSTRIP TRANSMISSION LINES

J. L. Gómez Tornero and A. Álvarez Melcón
Technical University of Cartagena
Campus Muralla del Mar s/n, 30202 Spain

Received 19 October 2002

ABSTRACT: *In this paper the leakage effects in open laterally-shielded multilayered microstrip transmission lines are investigated. Potential solutions are often reported to be difficult to find, since they are located in the complex propagating factor plane. To overcome this problem, a novel iterative algorithm is implemented to relate the solutions in the real axis of closed transmission lines with their corresponding complex open structure modes. The problem of modeling the leaky behavior of the open top wall is introduced, and a mathematical and physical explanation of the solutions is proposed. The advantage of this new technique is that it allows us to easily track the leaky solutions to their final location in the complex plane. Results are presented, including the field and power patterns associated to leaky waves, showing that the derived technique is indeed effective for the study of the complex modes excited in this type of structures.* © 2003 Wiley Periodicals, Inc. Microwave Opt Technol Lett 37: 88–93, 2003; Published online in Wiley InterScience (www.interscience.wiley.com). DOI 10.1002/mop.10832

Key words: *antennas; leaky waves; microstrip structures; numerical methods; integral equation*

1. INTRODUCTION

The leaky modes excited in open microstrip-like structures have been studied in the past by many researchers [1–13]. This radiation mechanism can be undesirable for printed-circuit applications, since it can cause interference and thus deteriorate the system performance. On the contrary, this radiation mechanism can be used in the design of leaky wave antennas [5, 11–13]. In any case, it is always convenient to control this leakage effect.

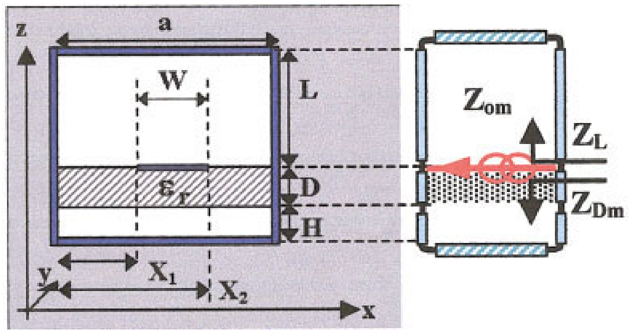

Figure 1 Cross section of the structure and equivalent network. [Color figure can be viewed in the online issue, which is available at www.interscience.wiley.com.]

The properties of the proposed solutions for microstrip configurations have also been mentioned in many papers, including the apparently growing amplitude behavior along the stratification axis [9]. However, how to mathematically treat this situation in order to retrieve the field pattern associated with leaky wave solutions is not easily found. The field associated to a leaky wave mode is computed in [6], but only over the metal strip, and no details are given as to how the field in the cross section can be evaluated. In addition, in [11–13] the field pattern is computed, but the leaky wave antenna is built using an empty waveguide with no dielectrics or printed metal strips. In the structure we propose, a suspended dielectric substrate is used in order to obtain a high gain behavior following similar ideas as those presented in [5].

Searching the complex poles of the leaky waves is also an interesting subject [8–10]. This is usually a complex task, since a search procedure must be implemented in a 2D complex plane. Yet, simple and efficient search strategies, which can be used to track the location of the complex leaky modes, are not generally found. For instance, in [10], the complex poles are found by taking as initial point in the search algorithm the quasi-static asymptotic location of the solutions at low frequency [8]. In addition to these iterative strategies, graphical procedures to approximately locate the complex leaky wave poles have also been derived [9].

Also, although many investigations have been conducted for basic printed lines [1–10], the same is not generally true for laterally shielded configurations. In all previous works, the infinite nature of the dielectric substrates yields to continuous wavenumbers in the spectral domain. For the shielded version, however, the discrete nature of the wavenumber must be carefully treated.

In this paper, we propose to study for the first time the leaky effects of a laterally shielded suspended microstrip line (Fig. 1). In addition to the basic formulation, we propose a novel technique which can be used to easily track the leaky modes as they move to the complex plane. This is essentially achieved by relating the leaky wave modes of the open transmission line with the real propagating waves of the closed counterpart. Also, the technique implemented can treat the growing behavior of the modes along the stratification axis, and this has allowed to obtain for the first time the field and power density distributions associated with these leaky wave modes.

The studied structure and the method used are presented in section 2. The modes in a closed transmission line, what we call the dielectric-bounded and the dielectric-leaky regimes, are obtained for a given example and properties of both are presented. The real modes of the closed structure will then be used in the novel search procedure to find the complex leaky wave solutions of the open structure. This novel search procedure for the complex